doi:10.1016/j.jmb.2009.09.064 J. Mol. Biol. (2009) 394, 805–814

JMB

Available online at www.sciencedirect.com

ScienceDirect

ELSEVIER

A DNA-Assisted Binding Assay for Weak Protein–Protein Interactions

Katherine E. Frato† and Robert F. Schleif*

Department of Biology, Johns Hopkins University, 3400 North Charles Street, Baltimore, MD 21218, USA

Received 14 August 2009; received in revised form 21 September 2009; accepted 29 September 2009
Available online
6 October 2009

We describe a new method used for quantitating weak interactions between proteins in which the weak interaction is "assisted" by a known DNA–DNA interaction. Oligonucleotides, which are conjugated to proteins of interest, contain short complementary DNA sequences that provide additional binding energy for protein–protein interactions. A stretch of unpaired bases links the protein to the hybridizing DNA sequence to allow formation of both protein–protein and DNA–DNA interactions with minimal structural interference. We validated the DNA-assisted binding method using heterodimerizing coiled-coil proteins. The method was then used to measure the predicted weak interaction between two domains of the *Escherichia coli* L-arabinose operon regulatory protein AraC. The interaction between domains has the expected magnitude (K_d = 0.37 mM) in the absence of arabinose. Upon addition of arabinose, we detected a weaker and unexpected interaction, which may necessitate modification of the proposed mechanism of AraC. The DNA-assisted binding method may also prove useful in the study of other weak protein–protein interactions.

Keywords: AraC; protein interactions; domain–domain interactions; fluorescence; protein–DNA conjugation

Edited by J. O. Thomas

Introduction

Weak protein–protein interactions are ubiquitous in biological processes. Individual proteins in macromolecular complexes are held at a high effective local concentration by virtue of their mutual binding partners. Similarly, the domains of an individual protein are forced into a high effective local concentration as a consequence of their covalent linkage. The pairwise interactions between binding partners held at a high local concentration by any mechanism must be weak when processes such as ligand binding and phosphorylation dynamically regulate these interactions. Controlled low-affinity domain–domain interactions have been observed in bacterial two-component signaling proteins NarL[1] and CheA[2] and in the mammalian nucleotide exchange factor P-Rex1,[3] and have been suggested for the *Escherichia coli* transcription factor AraC.[4–6]

Quantitative measurements of the weak interactions between proteins or domains of a protein are critical for a deep understanding of the energetics of protein regulation. However, the AraC protein is not sufficiently soluble to allow the preparation of high-concentration samples for conventional biophysical measurements. To date, we have been unable to detect the predicted interaction between domains of AraC by NMR or surface plasmon resonance (M. Rodgers, N. Neumann, and R.F.S., unpublished results). We required a new method that would be able to measure weak interactions between proteins at tractable protein concentrations.

We have developed a quantitative method for measuring weak interactions between two proteins or protein domains. Oligonucleotides containing short complementary sequences are conjugated to the proteins of interest. Weak DNA hybridization provides additional binding energy for the protein–protein interaction. A stretch of unpaired bases links the protein to the hybridizing DNA sequence to allow formation of both protein–protein and DNA–DNA interactions with minimal structural interference. Because the two binding events are linked, the

**Corresponding author.* E-mail address: rfschleif@jhu.edu.
† Email address: kfrato@jhu.edu.

Abbreviations used: DBD, DNA-binding domain; EDTA, ethylenediaminetetraacetic acid; TCEP, tris(2-carboxyethyl)phosphine.

association of the conjugates is tighter than either individual interaction. The virtues of using DNA for both the flexible linker and the source of assisting binding energy are as follows: the interaction energy provided by DNA hybridization can be easily varied, and placement of a fluorophore and a fluorescent quencher on complementary DNA strands provides a convenient assay for association.

In this study, we employ heterodimerizing coiled coils to show that the DNA-assisted binding method follows theoretical expectations, and we demonstrate that the method can be used to extract a quantitative measure of the strength of the protein–protein interaction. We then use the method to test for the predicted arabinose-dependent interaction between the dimerization domain and the DNA-binding domain (DBD) of the *E. coli* transcription factor AraC.[4–6]

Results

General principles of DNA-assisted binding

Consider two weakly associating molecules A and B, which are each connected via a flexible linker to one of a pair of weakly associating molecules a and b. The association of the covalent conjugates A–a and B–b will be tighter than the binding of A to B or the binding of a to b. In the general scheme used in this study (Fig. 1), the weak interaction between proteins of interest is assisted by another weak interaction between two complementary single-stranded DNA sequences. We chose to use DNA for both the linker and the source of assisting interaction. Associating proteins and associating DNA sequences are connected with a flexible poly (dT) linker, which allows the DNA–DNA and protein–protein interactions to form without steric interference. Thymidine engages in limited hydrophobic stacking, making these sequences more flexible than random DNA sequences.[7,8]

The strength of the protein–protein interaction is related to the interaction strength of the protein–DNA conjugates by:

$$K_{\text{total}} = \frac{K_{\text{DNA}} K_{\text{protein}}}{C_{\text{eff}}} \quad (1)$$

where K_{total} is the equilibrium dissociation constant of the peptide–DNA conjugates, K_{DNA} is the equilibrium dissociation constant for the DNA components alone, K_{protein} is the equilibrium dissociation constant for the protein components alone, and C_{eff} is the effective local concentration of one protein in the presence of the other when the complementary DNA sequences are hybridized.[9–12]

The effective local concentration C_{eff} is a function of linker length and flexibility. Decreasing the linker length increases the effective local concentration and increases the coupling of the interactions. However, shorter linkers have the potential to introduce steric interference and may limit the rotational freedom of the binding partners to engage at the preferred interface. For nonideal linkers that are not completely flexible, such as poly(dT) DNA, the orientation of the linkers can in turn restrict the orientation of the binding partners, causing a decrease in the effective local concentration. The effective local concentration also determines the weakest interaction that can be detected by DNA-assisted binding. Any interaction weaker than the effective local concentration will not be significantly "assisted" by the DNA.

We experimentally determined the values of C_{eff} for several of the linker pairs used in this study by measuring the equilibrium dissociation constants for two identical short complementary DNA sequences connected by a pair of identical six-base poly(dT) linkers (T6-T6) or a pair of four-base and eight-base poly(dT) linkers (T4-T8) (Supplementary Fig. 2). We measured the strength of the complementary DNA–DNA interaction alone (K_{DNA}), as well as the combined interaction of the two identical complementary sequences when connected by either pair of the linkers (Supplementary Results). From these

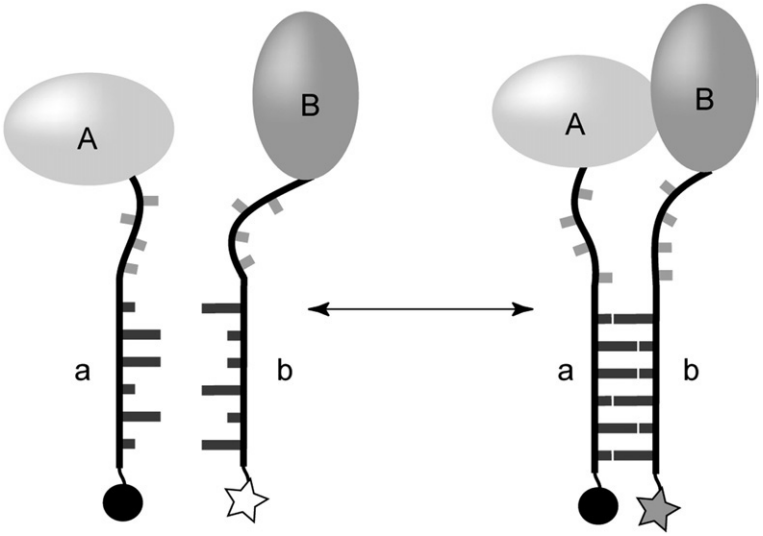

Fig. 1. Experimental design of a generic DNA-assisted binding experiment. In the generalized DNA-assisted binding experiment, A and B are proteins that interact weakly, and a and b are weakly hybridizing DNA oligomers. Light-gray bars denote the flexible linker, which could be poly(dT), abasic DNA, or short polyethylene glycol polymers. Black circles denote a generic quencher moiety, and stars denote a generic fluorophore. Fluorescence is quenched upon DNA–DNA association, as indicated by the gray star.

measurements, we calculated the C_{eff} for the T6-T6 linkers at 500 mM NaCl to be 2.0±1.1 mM, and that for the T4-T8 linkers at 300 mM NaCl to be 1.1± 0.3 mM. Theoretical values for C_{eff} estimated by assuming that the linkers are nonreplusive, fully flexible, and of zero diameter are within a factor of 3 of the values derived from the experiment (Supplementary Results). With decreasing salt concentration, the value of C_{eff} decreases sharply, presumably due to electrostatic repulsion between the phosphates of the DNA. Therefore, all our experiments were performed at monovalent salt concentrations of 300 mM or higher.

In DNA-assisted binding, the association of the protein–DNA conjugates can be measured by monitoring the spectroscopic signal of a fluorophore and a quencher placed on opposite DNA strands. DNA, unlike many proteins, can be inexpensively functionalized at defined locations that do not interfere with hybridization. Any pair of complementary fluorophores and quenchers could be used, and quenching moieties with large extinction coefficients and optimal spectral overlap with fluorophore emission will give a greater total signal change upon association. In these experiments, we chose 6-carboxyfluorescein as fluorophore and a pair of guanine bases as quencher. Guanine serves as a convenient quencher, as it can be inexpensively incorporated at both terminal location and interior location in a DNA oligomer. Guanine has been reported to quench a wide variety of fluorophores due to the transfer of an electron from the guanine base to the excited state of the fluorophore.[13–15] Preliminary DNA assistance experiments showed that a single overhanging guanine residue opposite the fluorophore is sufficient to give a quenching signal upon DNA hybridization, and additional overhanging guanines further increased the quenching of the fluorescence (data not shown).

Measuring a coiled-coil peptide interaction by DNA-assisted binding

To test the DNA-assisted binding method with proteins, we required a pair of associating proteins with known structure and for which the effect of salt concentration and pH on the association is known. A suitable choice is the K4-E4 heterodimerizing coiled-coil system, which has an equilibrium dissociation constant of 900 nM in 100 mM KCl at pH 7.[16] In each peptide, we substituted tryptophan for one residue at the N-terminus to facilitate concentration determination. Isothermal titration calorimetry experiments confirm that the equilibrium dissociation constant for the modified K4 and E4 peptides is approximately 1 μM in a buffer containing 500 mM NaCl at pH 8 (data not shown).

For the experiments with the associating coiled coils (Fig. 2), we chose complementary DNA sequences that interact very weakly, with a measured equilibrium dissociation constant K_{DNA} of 1900±100 nM. When linked by T6-T6 to the coiled-coil peptides, the interaction of the peptide–DNA conjugates (K_{total}) was 7±2 nM—260-fold tighter than the interaction of the DNA alone. Thus, the interaction of the peptides increased the apparent strength of the DNA–DNA interactions, as expected. Using Eq. (1) and the experimentally determined C_{eff} of 2.0 mM, the strength of the peptide–peptide interaction $K_{protein}$ is calculated to be 7000±2000 nM.

Confirmation of expected DNA-dependent effects

To verify that the binding of the protein–DNA conjugates obeys the relations in Eq. (1), we confirmed that the association depends on the effective local concentration. Lengthening the poly (dT) linker should decrease the effective local

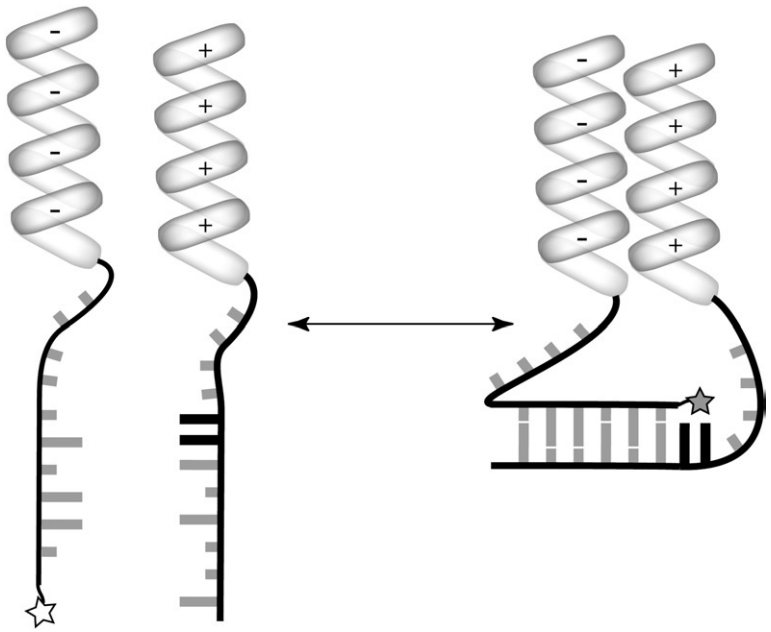

Fig. 2. Experimental design for measurement of the interaction between E4 and K4 coiled coils. The C-terminus of each peptide is conjugated to the 5′ end of a DNA oligomer. Poly(dT) sequences serve as the flexible linker between protein and hybridizing DNA. Black bars show the position of guanine bases that serve to quench the fluorescence upon binding.

concentration of the peptides, thereby weakening the affinity of the interaction between the two peptide–DNA conjugates. Simple geometrical estimates of C_{eff} based on the volume of space that is accessible to the linkers suggest that lengthening both linkers to T9 or T12 without changing $K_{protein}$ or K_{DNA} should decrease the affinity of the peptide–DNA conjugates to 19 nM or 42 nM (Supplementary Results). Measurements of the DNA-assisted coiled-coil interaction strength using a pair of T9 linkers and a pair of T12 linkers gave dissociation constants (K_{total}) of 16±2 nM and 26±7 nM, respectively, confirming that increasing the linker length decreased the affinity of peptide–DNA conjugate binding.

We also confirmed that different complementary DNA sequences with different interaction strengths result in appropriate changes in the measured interaction between the peptide–DNA conjugates. The interaction of hybridizing sequences with a single GC-to-AT substitution was calculated by nearest-neighbor methods[17] because the interaction was too weak for convenient experimental measurement. The single base-pair change was calculated to weaken the DNA–DNA interaction by 5-fold. When the GC-to-AT substituted DNA sequences were conjugated to the K4 and E4 peptides, we measured a 3-fold decrease in the interaction between the conjugates—a shift in K_{total} from 7±2 nM with the original DNA sequence to 24±10 nM. The difference between the expected change and the measured change in the interaction between conjugates is within the error of the computational estimates of weak hybridization between very short oligonucleotides.

The domain–domain interaction in AraC

We applied the DNA-assisted binding method to investigate an important biological concern: the mechanism of the AraC transcription factor in *E. coli*. The AraC monomer consists of two domains, an N-terminal dimerization domain which also binds sugars, and a C-terminal DBD, connected by a flexible linker.[18,19] A substantial body of genetic, physiological, and biophysical evidence suggests that AraC acts through a "light-switch" mechanism, where the major conformational change in the protein in response to arabinose is in the 18-residue N-terminal arm.[5,20–23] In the repressing state, the N-terminal arm binds both the dimerization domain and the DBD, holding the protein in a rigid conformation.[4,6,24] In the activating state, the arm binds over the arabinose-binding pocket. This is postulated to release the DBD to allow binding to adjacent DNA half-sites[4,25] (Fig. 3). The mechanism predicts an interaction between the DBD and the dimerization domain that is reduced or eliminated in the presence of arabinose.

The light-switch model for AraC action leads to the prediction that the domain–domain interaction

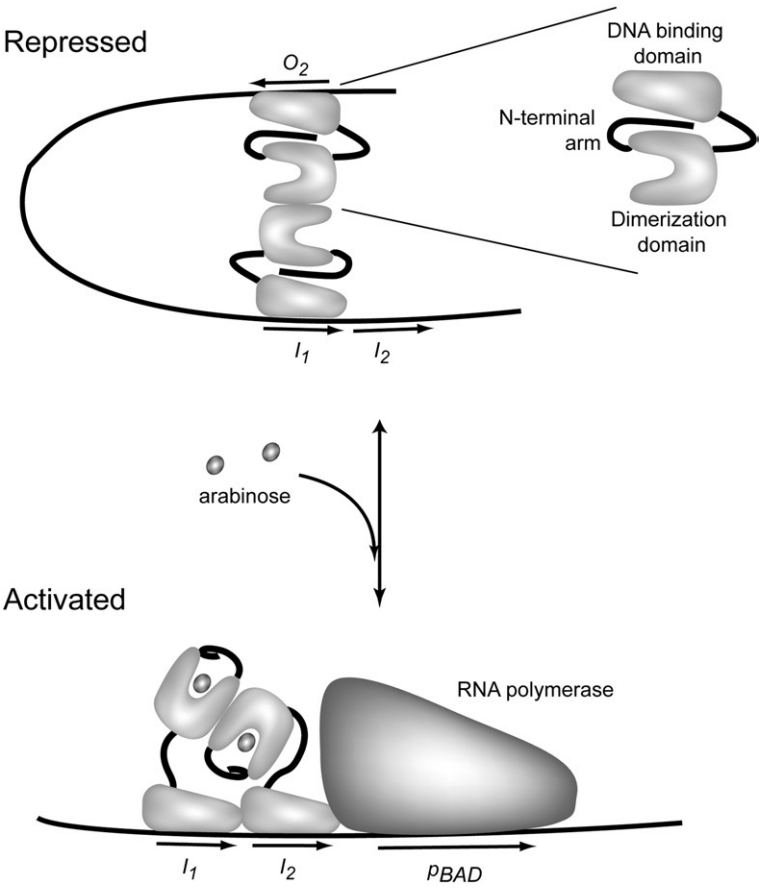

Fig. 3. Regulation of the p_{BAD} promoter by AraC. In the absence of arabinose, the AraC dimer binds to distant I_1 and O_2 half-sites, forming a DNA loop and repressing transcription of downstream genes. When arabinose is added, AraC protein undergoes a conformational change in the N-terminal arm that increases the flexibility of the dimer. Arabinose-bound AraC preferentially binds to adjacent I_1 and I_2 half-sites to activate transcription from the p_{BAD} promoter.

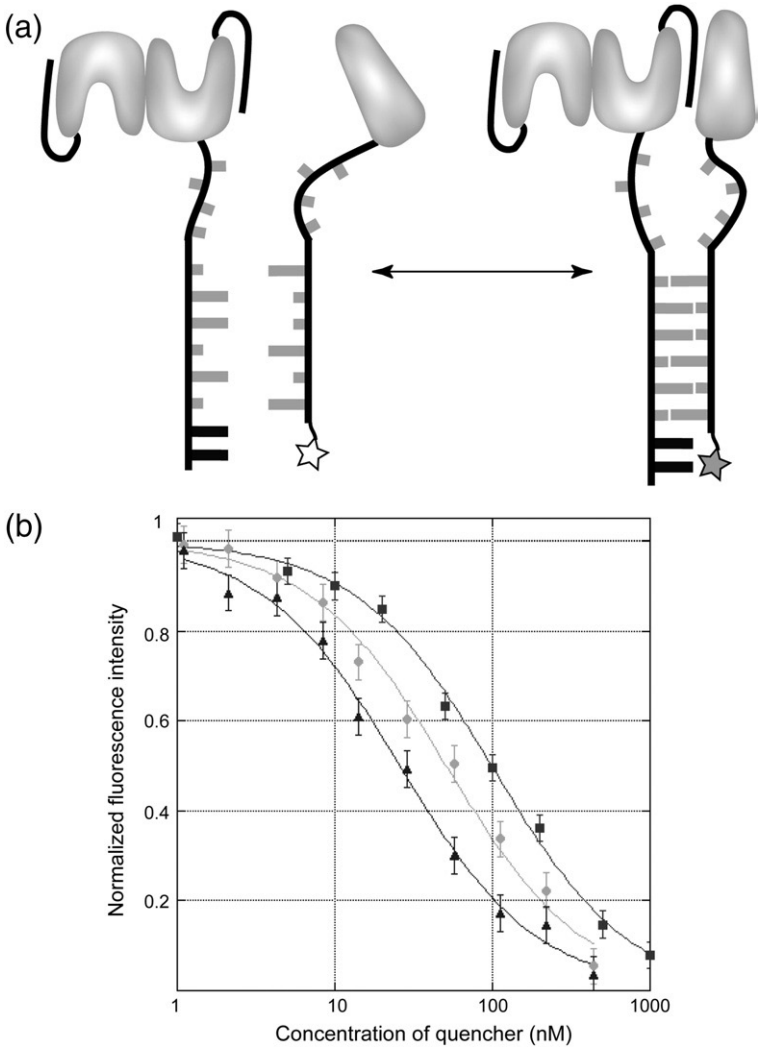

Fig. 4. The DNA-assisted binding assay measures an arabinose-dependent interaction between the dimerization domain and the DBD of AraC. (a) Experimental design for measurement of interaction between domains in AraC. Dimerization domain and DBD are each conjugated to a DNA oligomer. Black bars indicate the location of the two guanine residues that serve to quench the fluorophore in the bound state. Experiments were performed using singly conjugated dimers of the dimerization domain. (b) Binding of AraC domain–DNA conjugates as measured by a decrease in the normalized fluorescence intensity of the fluorophore. The control experiment (squares) measures the binding of the DBD–DNA conjugate to DNA alone. Circles show the binding of DBD–DNA conjugates to dimerization domain–DNA conjugates in the presence of arabinose. Triangles show the binding of DBD–DNA conjugates to dimerization domain–DNA conjugates in the absence of arabinose. Curves are a least-squares fit to each binding isotherm, as described in Materials and Methods.

in AraC will be extremely weak. Because the model requires that the two domains associate and dissociate in response to the signal provided by arabinose, the equilibrium dissociation constant between the domains of AraC must be on the same order of magnitude as the effective local concentration of one domain in the presence of the other domain *in vivo* (Supplementary Discussion). The eight-residue native interdomain linker in AraC[19,26,27] results in a 10 mM local concentration of one domain in the presence of the other . If the K_d between isolated domains were 1 μM, the domains in the context of native AraC would only dissociate and form the activating conformation 1:10,000th of the time, causing the AraC protein to be stuck in the repressing conformation. We therefore expect the interaction between the domains in the absence of arabinose to be extremely weak (between 0.1 mM and 1 mM). Such a weak interaction is near the limit of detection with our DNA-assisted binding method. In light of the expected marginal detectability of the domain–domain interaction in AraC, we used the shortest possible linkers compatible with the geometry of AraC: a T4 linker on the DBD and a T8 linker on the dimerization domain.

The DNA-assisted binding method succeeded in detecting an arabinose-regulated interaction between the domains of AraC (Fig. 4, Table 1). The data clearly show an interaction between the domains and a weakening of this interaction in the presence of arabinose. Control experiments were conducted to confirm that the change in the interaction is not a result of one of the individual domains affecting the DNA hybridization (see the text below). Application of Eq. (1) to the measured dissociation constants gives an interaction of 0.37±0.06 mM between the

Table 1. Equilibrium dissociation constants of AraC domain–DNA conjugates and effects of mutations on the interaction between AraC domains

Dimerization domain mutation	No Arabinose (nM)	Plus Arabinose (nM)
Wild type	31±4[a]	50±4
G12T	46±3	62±1
Δ8–14 (arm deletion)	65±5	62±4

The interaction of the DNA component alone is 92±8 nM.
[a] All reported errors are standard deviations of K_d values derived from at least three independent experiments.

domains in the absence of arabinose and a weaker interaction of 0.60±0.07 mM between the domains in the presence of arabinose. This result is highly reproducible. Experiments performed months apart and with different preparations of the conjugates show the same differences between binding with arabinose and binding without arabinose, and when compared to the DNA-only control.

Effect of constitutive mutations on AraC domain interactions

In the absence of arabinose, the DBD of AraC appears to be rigidly held to the dimerization domain, leading to repression; in the presence of arabinose, the DBD appears to be released from the dimerization domain, leading to induction.[4,6,25] Mutations could therefore exist where the interaction between domains is weakened and the protein cannot form a rigid repressing structure. These mutations would display a constitutive phenotype—they would no longer need arabinose to induce. Indeed, constitutive mutations in AraC have been isolated and studied.[5,23,28–31]

We tested whether constitutive mutations in AraC decrease the strength of the interaction between the dimerization domain and the DBD. The mutant AraC G12T displays an intermediate constitutive phenotype,[30] and we predict that the mutant protein will possess a partial defect in the interaction between domains. The G12T mutant decreased, but did not eliminate, the interaction between domains both in the presence and in the absence of arabinose (Table 1).

We expect that deletion of residues 8–14 in the N-terminal arm, which results in a full constitutive phenotype, will eliminate the minus-arabinose interaction between the domains. Deletion of the arm did eliminate, as predicted, the specific minus-arabinose interaction (Table 1). However, it left the interaction between domains seen in the presence of arabinose.

Experimental controls on effects of protein–DNA conjugation

We performed a number of control experiments to test for possible artifacts. Arabinose binding and I_1 DNA binding assays confirmed that the dimerization domain and the DBD remained active after conjugation to DNA. The dimerization domain–DNA conjugate binds arabinose with the same affinity as for the unconjugated dimerization domain. Similarly, the change in the average emission wavelength of the intrinsic tryptophan fluorescence upon arabinose binding is unchanged by DNA conjugation. The DBD remains competent to bind I_1 half-site DNA when conjugated, although at least 10-fold-higher concentrations of DBD–DNA conjugate are required to detect binding via a gel retardation assay (data not shown). This difference is not unexpected, as the conjugated DNA adds a substantial negative charge that likely interferes with I_1 DNA binding.

It is possible that the addition of arabinose to the DNA assistance experiments could perturb the hybridization of the DNA. To control for this effect, we conducted experiments with arabinose, with glucose, or without sugar and showed that the DNA hybridization is not affected by the presence of different sugars (data not shown). This confirms that the weakening of the protein–DNA conjugate interaction by the addition of arabinose is not a consequence of the sugar weakening the DNA–DNA interaction.

Because proteins conjugated to DNA could perturb the DNA hybridization interaction, we also showed that neither the DBD nor the dimerization domain affects the hybridization of the conjugated DNA. The binding between DBD–DNA conjugate and DNA alone, as well as the binding between dimerization domain–DNA conjugate and DNA alone, is the same as the DNA hybridization in the absence of any protein conjugate. Furthermore, the binding of dimerization domain–DNA conjugate to DNA is unchanged by arabinose.

Discussion

Weak protein–protein interactions are widespread in biology because many proteins function as members of large macromolecular complexes such as ribosomes, spliceosomes, fatty acid synthases, and transcription enhancer complexes. In these complexes, individual proteins are held at a high local concentration; thus, pairwise interactions between proteins need only to be weak to build a strong network of interacting proteins. Weak interactions can also be found between the domains of an individual protein, which are held at a high local concentration as a consequence of their covalent linkage. In one such example (the regulatory protein AraC), it is predicted that the weak interaction between the domains will be further weakened or eliminated by the addition of arabinose.[4–6] The weakness of this interdomain interaction has thus far prevented its detection and quantitation with *in vitro* biophysical methods. In this study, we developed the DNA-assisted binding method to detect and measure the predicted weak domain–domain interaction in AraC and to show that it is further weakened by the addition of arabinose. The method should be useful in the study of weak interactions in other systems.

Our *in vitro* DNA-assisted binding method makes weak protein–protein interactions easier to measure by helping to bring the binding partners into high effective local concentration. We use DNA hybridization as the source of additional binding energy. This allows the assay to be quantitative, as energetic contributions from the DNA interaction can be accurately measured or calculated. Furthermore, the strength of the DNA contribution is tunable by changing DNA sequence, salt concentration, or temperature. DNA can be inexpensively and specifically functionalized, allowing for simple detection

of the interaction through fluorescence quenching. Finally, the *in vitro* nature of the experiment allows the interaction to be measured in a controlled environment (e.g., in the presence or in the absence of other molecules that modulate the interaction).

We used a model system of dimerizing coiled coils to prove the applicability and quantitative rigor of the DNA-assisted binding assay. The coiled-coil interaction does indeed strengthen the interaction of the peptide–DNA conjugates as compared to the DNA interaction alone (from 1900 nM for DNA alone to 7 nM with the peptide–DNA conjugates). This corresponds to a coiled-coil interaction with a K_d of 7000±2000 nM, which agrees reasonably well with the affinity of the K4 and E4 in our sample buffer. We further confirmed that the affinity of the peptide–DNA conjugates varies with the strength of the DNA hybridization and the length of the flexible DNA linker, as predicted.

We employed the DNA-assisted binding method to investigate the mechanism of the AraC protein. We directly verified, as predicted by a wealth of indirect experimental data,[4–6,18–24] an interaction between the dimerization domain and the DBD with a K_d of about 0.37 mM, and we showed that this interaction is weakened by arabinose. Unexpectedly, we found a residual interaction between the domains that remained despite the presence of arabinose. This plus-arabinose interaction was also present in a mutant where the N-terminal arm, which is required for the interaction between domains, is deleted. Below, we-consider two possible interpretations of the plus-arabinose interaction. First, we consider the possibility that the plus-arabinose interaction is functionally relevant, and we review its implications for the current model for AraC action. We then consider the possibility that the residual interaction is not directly related to AraC function, but represents a nonspecific domain–domain interaction of a type that may exist between many protein pairs.

First, let us assume that the plus-arabinose interaction is functionally relevant. By comparing our measured domain–domain interactions with the difference in energy between the arabinose-bound state and the arabinose-free state in the intact protein, we can determine whether the measured change in the domain–domain interaction is sufficient to account for the regulatory behavior of the intact protein. In the light-switch model, AraC is only able to bind to adjacent DNA half-sites when the arm-mediated domain–domain interaction has been released. Several lines of evidence suggest that the addition of arabinose increases by 40-fold the amount of AraC that is capable of binding to adjacent DNA half-sites[25,32–34] (Supplementary Discussion). This corresponds to a 2.1 kcal/mol difference between the arabinose-bound state and the arabinose-free state. If only one monomer of AraC must change conformation to shift the dimer to the inducing state, a single monomer should account for the 2.1 kcal/mol change in free energy between states. However, if both monomers must change conformation to shift the dimer into the inducing state, the energy difference is divided between both monomers, giving a 1.1 kcal/mol difference. Our observed change in equilibrium dissociation constant between the domains of a single monomer (from 0.6 mM in the presence of arabinose to 0.37 mM in the absence of arabinose) corresponds to a 0.27 kcal/mol difference between the arabinose-bound state and the arabinose-free state. Thus, the mechanism currently proposed for AraC may be incomplete, in which case as-yet-undetected arabinose-dependent conformational changes must be required to switch the protein to an activating state.

An alternative possibility is that the domain–domain interaction that remains in the presence of arabinose is a result of one or more nonspecific interactions that have little or nothing to do with normal AraC function. For example, they could result from an interaction that is prevented by the native interdomain linker present in intact AraC. If this is true, it is possible that many pairs of proteins have weak nonspecific interactions that are irrelevant to biological function. The DNA-assisted binding method could serve as a way to investigate this class of weak protein–protein interaction.

The DNA-assisted binding method is particularly well suited to the measurement of small changes in the strength of a weak interaction. In a system where the interaction interface and linkers remain the same, sources of systematic error, such as uncertainty in C_{eff}, cancel out. In these cases, as seen in the investigation of the AraC domain–domain interaction (Table 1), the assay generates highly reproducible data with small errors. We expect therefore that the DNA-assisted binding assay will prove particularly useful in studying the effects of ligands and mutations on weak interactions in other systems.

In this study, we developed a method to measure weak protein–protein interactions using protein–DNA conjugates. We used this method to measure the interaction between the domains of the AraC protein in the absence of arabinose, confirming a prediction of the light-switch mechanism. We also detected a weak interaction between the two domains of the AraC protein in the presence of arabinose. The plus-arabinose interaction is not predicted by the light-switch mechanism and suggests the presence of an additional as-yet-undiscovered component to the protein's arabinose response.

Materials and Methods

DNA for intein-mediated conjugation

All DNA oligonucleotides used for intein-based conjugation were functionalized at the 5′ end with Oligo-Modifying Reagent (Glen Research) and synthesized at the DNA/RNA Synthesis Core Facility at the Johns Hopkins School of Public Health. Fluorescent DNA oligonucleotides were further modified at the 3′ end with 6-carboxyfluorescein. Synthetic oligonucleotides

resuspended in 10 mM Tris (pH 8) and 1 mM ethylenediaminetetraacetic acid (EDTA) were deprotected with at least 5 mM tris(2-carboxyethyl)phosphine (TCEP; Thermo Scientific) at room temperature for at least 30 min immediately before conjugation.

DNA sequences of assisting oligomers

The oligomers used in the coiled-coil experiments were 5′-TTTTTTGG**GTTCTAC**-3′ and 5′-TTTTTT**GTAGAAC**-3′, as well as the GC-to-AT substituted sequences 5′-TTTTTTGG**GTTATAC**-3′ and 5′-TTTTTT**GTATAAC**-3′ (complementary sequences in boldface). The oligomers for the AraC domain interaction experiments were 5′-TTTT**GTCGAAC**-3′ and 5′-GG**GTTCGAC**TTTTTTTT-3′.

Design of coiled-coil DNA conjugates

Because the K4 and E4 peptides were expressed and purified as intein fusions to allow intein-mediated DNA conjugation, we slightly modified the original K4 and E4 peptide sequences.[16] An N-terminal methionine allows the peptide to be expressed in *E. coli*. Addition of an alanine residue between the peptide and the intein fused to the C-terminus of the peptide increases the rate of cleavage by the intein.[35] A valine-to-tryptophan substitution near the N-terminus of both peptides allows the concentration to be determined by absorption at 280 nm. The sequences were K4, MAKWSALKEKVSALKEKVSALKEKVSALKEAA and E4, MAEWSALEKEVSALEKEVSALEKEVSALEKAA.

The concentration of peptide–DNA conjugates was determined by absorbance at 260 nm. Extinction coefficients were calculated as absorbance at 260 nm for the DNA alone, added to the absorbance of the single tryptophan at 260 nm (3750 M^{-1} cm^{-1}). The molar extinction coefficient for the T6-linked K4–DNA conjugate with hybridizing DNA sequence 5′-GTTCTAC-3′ was 132,100 M^{-1} cm^{-1}, and all other extinction coefficients were calculated similarly.

Cloning and purification of coiled-coil peptide–DNA and DBD–DNA conjugates

DNA coding for the K4 and E4 peptides was synthesized by Integrated DNA Technologies. DNA coding for the AraC DBD (AraC amino acid residues 175–292) was modified by QuikChange site-directed mutagenesis (Stratagene) to remove the final 11 residues of the DBD, which have been shown by NMR to be unstructured and are not required for AraC repression or induction.[19,27] Coding DNA was then cloned into the pTXB3 vector (New England Biolabs) using NcoI and SapI sites. Proteins were expressed as intein fusions in *E. coli* BL21(DE3) cells and purified using chitin beads (New England Biolabs) in accordance with the manufacturer's protocol.[36] Cleavage of the peptide or protein from the intein was initiated by the addition of sodium-2-sulfanylethanesulfonate up to 50 mM. DBD–intein fusions were incubated for 3 h at room temperature, and coiled-coil peptide–intein fusions were incubated overnight at room temperature. Free sodium-2-sulfanylethanesulfonate-activated proteins were eluted and concentrated to approximately 1 mL using Amicon Ultra-4 Centrifugal Filters.

Coiled-coil peptides (500 μM) were added in at least 4-fold molar excess to deprotected 5′-cysteinyl-modified DNA and allowed to react overnight at room temperature in a final volume of 1 mL. Peptide–DNA conjugates were purified by binding to a 1-mL butyl-HP column (GE Biosciences) and eluted with an ammonium sulfate gradient (2– 0 M). The purity of fluorescent peptide–DNA conjugates was assessed by SDS-PAGE, followed by visualization of fluorescent bands. The presence of peptides in the conjugate was confirmed by tryptophan fluorescence of column fractions. Peptide–DNA conjugates were dialyzed overnight in 0.8 M NaCl, 20 mM Tris (pH 8), and 1 mM EDTA in a dialysis tubing with a 500-Da molecular mass cutoff and stored at room temperature. Concentration was determined by absorbance at 260 nm.

DBD (200 μM) was reacted overnight in approximately 1.5 mL with a 2:1 molar ratio of DBD to deprotected 5′-cysteinyl-modified fluorescent DNA. DBD–DNA conjugates were purified by binding to 1-mL heparin HP columns (GE Healthcare) and eluting with a gradient from 0.05 M to 1 M NaCl in 20 mM sodium phosphate (pH 6), 1 mM EDTA, and 1 mM DTT.

Purification and conjugation of the AraC dimerization domain

Purification of the Y31V, C66S, and S170C AraC dimerization domain using the pET21-based AraCTF vector[37] was performed as previously described.[26] The dimerization domain was conjugated to DNA with sulfosuccinimidyl-4-(*N*-maleimidomethyl)cyclohexane-1-carboxylate (Pierce Biotechnology). DNA oligomers with 3′ primary amine groups were purchased from Integrated DNA Technologies. Crosslinker and DNA were mixed in a 20:1 molar ratio (total volume, 300 μL) in 100 mM sodium phosphate (pH 7.5) and 1 mM EDTA, and reacted at room temperature for 3 h. Excess crosslinker was removed by buffer exchange through G-10 size-exclusion beads twice. The dimerization domain was incubated with 10 mM TCEP for 30 min and then transferred into a buffer containing 100 mM sodium phosphate (pH 7.5) and 1 mM EDTA by passage through G-10 size-exclusion beads twice. Sulfosuccinimidyl-4-(*N*-maleimidomethyl)cyclohexane-1-carboxylate-linked DNA and dimerization domain were mixed in a 2-fold molar excess of protein (total volume, 1.2 mL) and incubated overnight at room temperature. Protein–DNA conjugates were purified by two cycles of ammonium sulfate precipitation, followed by ion-exchange chromatography (volume, 1 mL; Pharmacia MonoQ HR 5/5) with a gradient from 0.05 M to 1 M NaCl. The singly conjugated dimer peak was pooled and dialyzed for 2 h and again overnight, each time in 500 mL of buffer containing 300 mM NaCl, 10 mM Tris (pH 8), and 0.5 mM EDTA to remove arabinose.

Determination of the concentration of AraC domain–DNA conjugates

The concentrations of both DBD–DNA and dimerization domain–DNA conjugates were determined by absorbance at 260 nm, where the majority of the absorbance is contributed by the DNA and the tryptophans in the protein. For dimerization domain conjugates, only one of the monomers in the dimer was conjugated to DNA (Supplementary Discussion); thus, molar extinction coefficients per dimer were calculated as the absorption of the DNA oligomer at 260 nm added to the contribution of tryptophans from two monomers (10 tryptophans in total) at 260 nm (3750 M^{-1} cm^{-1}). The molar extinction coefficients used were 187,900 M^{-1} cm^{-1} for dimerization domain-T8 and 105,150 M^{-1} cm^{-1} for DBD-T4.

Isothermal titration calorimetry

Isothermal titration calorimetry experiments were conducted in a VP-ITC (MicroCal) at 24 °C. K4 and E4 peptides were dialyzed overnight into an identical buffer containing 500 mM NaCl, 20 mM Tris (pH 8), and 1 mM EDTA. K4 peptide at 75 μM was placed in the cell, and 300 μM E4 peptide was placed in the syringe. Experiments consisted of 28 injections of 10 μL each at a rate of 0.5 μL/s, and 400 s elapsed between each injection. Data were analyzed using the Origin software package (MicroCal).

Fluorescence quenching measurements and analysis

Fluorescence measurements were made on a T-configuration Photon Technology International fluorimeter equipped with a 70-W xenon arc lamp light and a temperature-controlled cuvette holder. Experiments were conducted at 24 °C for coiled-coil measurements and at 20 °C for AraC domain measurements, in 5 mm pathlength quartz cuvettes. Coiled-coil experiments used a buffer containing 500 mM NaCl, 20 mM Tris (pH 8), 1 mM EDTA, 100 μg/mL bovine serum albumin, and 1 mM TCEP, and AraC experiments used a buffer containing 300 mM NaCl, 10 mM Tris (pH 8), 0.5 mM EDTA, 50 μg/mL bovine serum albumin, 2 mM $MgCl_2$, and 0.5 mM TCEP. When included, sugars were diluted from a 1 M sterile filtered stock to a final concentration of 10 mM. Mixtures of fluorophore and quencher conjugates (total volume, 750 μL) were preincubated for at least 1 h before fluorescence measurement. Samples were excited at 495 nm, and an emission spectrum was collected from 505 nm to 540 nm. Intensity was averaged from 515 nm to 540 nm and corrected for dilution due to the added volume of the quenching species. Average intensities were then fitted to a simple binding model:

$$\theta = \frac{Q}{K_d + Q} \quad (2)$$

where θ is the fraction bound and Q is the concentration of the quencher species. For several DNA control experiments and all coiled-coil conjugate experiments, where K_d was on the same order as the fluorophore concentration, we used the binding model:

$$\theta = (F_t + Q_t + K_d) - \sqrt{\frac{(F_t + Q_t + K_d)^2 - 4F_tQ_t}{2F_t}} \quad (3)$$

where θ is the fraction bound, F_f is the total fluorophore concentration, and Q_t is the total quencher concentration.

Acknowledgements

This work was supported by National Institutes of Health grant GM018277 to R.F.S. We thank Evan Brower and Ernesto Freire for assistance with isothermal titration calorimetry experiments. We also thank Michael Rodgers, Jennifer Seedorff, and Stephanie Dirla for assistance, discussions, and comments on this manuscript.

Supplementary Data

Supplementary data associated with this article can be found, in the online version, at doi:10.1016/j.jmb.2009.09.064

References

1. Eldridge, A. M., Kang, H.-S., Johnson, E., Gunsalus, R. & Dahlquist, F. W. (2002). Effect of phosphorylation on the interdomain interaction of the response regulator, NarL. *Biochemistry*, **41**, 15173–15180.
2. Hamel, D. J., Zhou, H., Starich, M. R., Byrd, R. A. & Dahlquist, F. W. (2006). Chemical-shift-perturbation mapping of the phosphotransfer and catalytic domain interaction in the histidine autokinase CheA from *Thermatoga maritima*. *Biochemistry*, **45**, 9509–9517.
3. Urano, D., Nakata, A., Mizuno, N., Tago, K. & Itoh, H. (2008). Domain–domain interaction of P-Rex1 is essential for the activation and inhibition by G protein βγ subunits by PKA. *Cell. Signalling*, **20**, 1545–1554.
4. Seabold, R. R. & Schleif, R. F. (1998). Apo–AraC actively seeks to loop. *J. Mol. Biol.* **278**, 529–538.
5. Saviola, B., Seabold, R. & Schleif, R. F. (1998). Arm–domain interactions in AraC. *J. Mol. Biol.* **278**, 539–548.
6. Rodgers, M. E., Holder, N. D., Dirla, S. & Schleif, R. (2009). Functional modes of the regulatory arm of AraC. *Proteins*, **74**, 81–91.
7. Mills, J. B., Vacano, E. & Hagerman, P. J. (1999). Flexibility of single-stranded DNA: use of gapped duplex helices to determine the persistence lengths of poly(dT) and poly(dA). *J. Mol. Biol.* **285**, 245–257.
8. Murphy, M. C., Rasnik, I., Cheng, W., Lohman, T. M. & Ha, T. (2004). Probing single-stranded DNA conformational flexibility using fluorescence spectroscopy. *Biophys. J.* **86**, 2530–2537.
9. Crothers, D. M. & Metzger, H. (1972). The influence of polyvalency on the binding properties of antibodies. *Immunochemistry*, **9**, 341–357.
10. Creighton, T. E. (1993). Proteins—Structures and Molecular Properties W. H. Freeman and Co., New York, NY.
11. Klemm, J. D. & Pabo, C. O. (1996). Oct-1 POU domain–DNA interactions: cooperative binding of isolated subdomains and effects of covalent linkage. *Genes Dev.* **10**, 27–36.
12. Schleif, R. & Wolberger, C. (2004). Arm–domain interactions can provide high binding cooperativity. *Protein Sci.* **13**, 2829–2831.
13. Heinlein, T., Knemeyer, J.-P., Piestert, O. & Sauer, M. (2003). Photoinduced electron transfer between fluorescent dyes and guanosine residues in DNA-hairpins. *J. Phys. Chem.* **107**, 7957–7964.
14. Noble, J. E., Wang, L., Cole, K. D. & Gaigalas, A. K. (2005). The effect of overhanging nucleotides on fluorescence properties of hybridizing oligonucleotides labeled with Alexa-488 and FAM fluorophores. *Biophys. Chem.* **113**, 255–263.
15. Lakowicz, J. (2006). Principles of Fluorescence Spectroscopy Springer, New York, NY.
16. Litowski, J. R. & Hodges, R. S. (2002). Designing heterodimeric two-stranded α-helical coiled-coils: effects of hydrophobicity and α-helical propensity on protein folding, stability, and specificity. *J. Biol. Chem.* **277**, 37272–37279.
17. Markham, N. R. & Zuker, M. (2005). DINAMelt web

server for nucleic acid melting prediction. *Nucleic Acids Res.* **33**, 577–581.
18. Bustos, S. A. & Schleif, R. F. (1993). Functional domains of the AraC protein. *Proc. Natl Acad. Sci. USA*, **90**, 5638–5642.
19. Eustance, R. J., Bustos, S. A. & Schleif, R. F. (1994). Reaching out: locating and lengthening the interdomain linker in AraC protein. *J. Mol. Biol.* **242**, 330–338.
20. Soisson, S. M., MacDougall-Shackleton, B., Schleif, R. & Wolberger, C. (1997). Structural basis for ligand-regulated oligomerization of AraC. *Science*, **276**, 421–425.
21. Harmer, T., Wu, M. & Schleif, R. (2001). The role of rigidity in DNA looping–unlooping by AraC. *Proc. Natl Acad. Sci. USA*, **98**, 427–431.
22. Wu, M. & Schleif, R. (2001). Strengthened arm–dimerization domain interactions in AraC. *J. Biol. Chem.* **276**, 2562–2564.
23. Wu, M. & Schleif, R. (2001). Mapping arm–DNA-binding domain interactions in AraC. *J. Mol. Biol.* **307**, 1001–1009.
24. Reed, W. L. & Schleif, R. F. (1999). Hemiplegic mutations in AraC protein. *J. Mol. Biol.* **294**, 417–425.
25. Carra, J. & Schleif, R. (1993). Variation of half-site organization and DNA looping by AraC protein. *EMBO J.* **12**, 35–44.
26. Weldon, J. E., Rodgers, M. E., Larkin, C. & Schleif, R. F. (2007). Structure and properties of a truly apo form of AraC dimerization domain. *Proteins*, **66**, 646–654.
27. Rodgers, M. E. & Schleif, R. (2009). Solution structure of the DNA binding domain of AraC protein. *Proteins*, **77**, 202–208.
28. Englesberg, E., Irr, J., Power, J. & Lee, N. (1965). Positive control of enzyme synthesis by gene C in the arabinose system. *J. Bacteriol.* **90**, 946–957.
29. Nathanson, N. M. & Schleif, R. (1973). A novel mutation to dominant fucose resistance in the L-arabinose operon of *Escherichia coli*. *J. Bacteriol.* **115**, 711–713.
30. Ross, J. J., Gryczynski, U. & Schleif, R. (2003). Mutational analysis of residue roles in AraC function. *J. Mol. Biol.* **328**, 85–93.
31. Dirla, S., Chien, J. Y.-H. & Schleif, R. (2009). Constitutive mutations in *E. coli* AraC protein. *J. Bacteriol.* **191**, 2668–2674.
32. Kolodrubetz, D. & Schleif, R. (1981). Identification of araC protein on two-dimensional gels, its *in vivo* instability and normal level. *J. Mol. Biol.* **149**, 133–139.
33. Hendrickson, W. & Schleif, R. F. (1984). Regulation of the *Escherichia coli* L-arabinose operon studied by gel electrophoresis DNA binding assay. *J. Mol. Biol.* **178**, 611–628.
34. Huo, L., Martin, K. J. & Schleif, R. (1988). Alternative DNA loops regulate the arabinose operon in *Escherichia coli*. *Proc. Natl Acad. Sci. USA*, **85**, 5444–5448.
35. Southworth, M. W., Amaya, K., Evans, T. C., Xu, M. -Q. & Perler, F. B. (1999). Purification of proteins fused to either the amino or carboxy terminus of the *Mycobacterium xenopi* gyrase A intein. *Biotechniques*, **27**, 110–120.
36. Evans, T. C., Benner, J. & Xu, M.-Q. (1998). Semi-synthesis of cytotoxic proteins using a modified protein splicing element. *Protein Sci.* **7**, 2256–2264.
37. LaRonde-LeBlanc, N. & Wolberger, C. (2000). Characterization of the oligomeric states of wild type and mutant AraC. *Biochemistry*, **39**, 11593–11601.